Application of powdered activated carbon coated with zinc oxide nanoparticles prepared using a green synthesis in removal of Reactive Blue 19 and Reactive Black-5: adsorption isotherm and kinetic models

Yousef Rashtbari[a,b], Shirin Afshin[a,b], Asghar Hamzezadeh[b], Malek Abazari[b], Yousef Poureshgh[b,*], Mehdi Fazlzadeh[b,c,*]

[a]*Students Research Committee, Faculty of Health, Ardabil University of Medical Sciences, Ardabil, Iran, Tel. +989383162079; email: u3f.rashtbari@gmail.com (Y. Rashtbari), Tel. +98 9014515339; email: shirinafshin1990@gmail.com (S. Afshin)*
[b]*Department of Environmental Health Engineering, School of Public Health, Ardabil University of Medical Sciences, Ardabil, Iran, Tel. +989148092356; emails: yusef.poureshg@gmail.com (Y. Poureshgh), m.fazlzadeh@gmail.com (M. Fazlzadeh), Tel. +98 9143540015; emails: a.hamzezade@yahoo.com (A. Hamzezadeh), abazari.malek@gmail.com (M. Abazari)*
[c]*Department of Environmental Health Engineering, School of Public Health, Tehran University of Medical Sciences, Tehran, Iran*

ABSTRACT

Dyes considered as a main environmental pollutant are present in various effluents released from different industries like textiles. Dyes cause problems such as reduced light penetration, allergies, and cancer when they are entered into the environment. The purpose of this study was to compare the efficiency of the activated carbon coated with the zinc oxide (ZnO) nanoparticles prepared by walnut shell in removing two dyes from aqueous environments. The study used a floating method to prepare the AC-ZnO composite. The composite structure and morphology were studied using Fourier transform infrared spectroscopy, Brunauer–Emmett–Teller (BET), X-ray diffraction and field emission scanning electron microscopy techniques. The results confirmed the accuracy of the composite structure. Moreover, the study examined reaction time, solution pH, composite volume, and initial dye concentration and AC-ZnO composite recovery. The removal efficiencies under the optimal conditions for Reactive Blue 19 (RB-19) and Reactive Black-5 (RB-5) (dye concentrations 100 mg L^{-1}, composite dose 1.5 g L^{-1}, reaction time 45 min and pH 3) were 97.36% and 73.36%, respectively. The results of the experimental data were fitted well to the Langmuir isotherm, indicating monolayer adsorption of both metal ions onto the AC-ZnO composite and an estimated adsorptive capacity of 71.42 (RB-5) and 94.33 mg g^{-1} (RB-19). However, the kinetic data agreed well with the pseudo-second-order model. The S_{BET} and total pure volume for the AC-ZnO composite and AC were 728.17 m^2 g^{-1}, 687.95 m^2 g^{-1} and 0.684 cm^3 g^{-1}, 0.612 cm^3 g^{-1}, respectively. It can be concluded that AC-ZnO composite as an effective and environmentally friendly adsorbent had a high ability in removing dye from aqueous solutions.

Keywords: Walnut shell; Scrap tires; Green synthesis; ZnO nanoparticle; Dye

1. Introduction

Nowadays, dyes have made major concerns about environmental pollution, particularly in effluents released from industries [1,2] such as textiles, food, paper, cosmetics, medicine, and leather [3,4]. In textile industries, about 10%–15% of the dyes make serious environmental problems after dyeing processes [5,6]. Most of the dyes in the wastewater are stable and non-biodegradable [7]. By limiting

* Corresponding authors.

the penetration of sunlight, dyes affect the photosynthetic capacity of aquatic plants [8,9]. Some dyes have toxic, carcinogenic and mutagenic impacts and affect human being's and animal's health [10]. The risks of dyes on the environment have made researchers focus on dye removal. In the last few decades, several methods such as filtration [11], biological purification [12,13], coagulation, and flocculation [14] and chemical oxidation have been developed [15] but each one has its disadvantages. Membranes applied for reverse osmosis processes are extremely expensive and contaminated membranes require special treatments for their recovery [16]. Coagulation and flocculation have limitations for the removal of dyes from wastewater due to their low capacity and production of large quantities of dangerous sludge [17]. Among the mentioned methods, the adsorption process is one of the most effective processes for dye removal at large scales [18–23].

There are several methods for the synthesis of nanoparticles. Many techniques are inefficient in terms of energy and material consumption. In most chemical methods, a chemical reducing agent is used as a stabilizer (polyvinylpyrrolidone) to control particle growth and prevent accumulation. Thus, the synthesis of environmentally friendly nanoparticles is increasing nowadays. An alternative method is to synthesize nanoparticles using biological methods. In this method, various plant extracts and their products can be used as an alternative to the synthesis of nanoparticles. Recently, plant extracts, such as green and black tea extracts, grape leaf and eucalyptus leaves, have been utilized to synthesize nZVI and other nanoparticles [24,25].

Among nanoparticles, zinc oxide nanoparticles (ZnO NPs) are one of the multifunctional inorganic nanoparticles considered as an ideal agent having many significant features [26]. In addition, human beings exposed to chemically synthesized ZnO NPs with smaller doses have not had toxic effects in vivo, whereas high concentrations can cause sudden death [27]. Furthermore, wide applications of ZnO NPs increase the potential toxic risk for its release to the environment [28]. Based on the biological method, the synthesis of the ZnO NPs benefits from simplicity, eco-friendliness and extended antimicrobial activity [29]. However, the nanoparticles produced by plants are more stable and the increased synthesis rate of nanoparticles attains a great interest due to crude extracts of plants containing a naturally occurring, reducing and stabilizing agent, making this an advantageous approach [30].

In the application of nanomaterials in filtration technology, the separation of dispersed nanoparticles from aqueous solutions at the end of the process is difficult. Thus, to accelerate the separation of them, the stabilization of the nanoparticles with materials such as oxides, polymers, fibers, activated carbon, and others are needed. Additionally, given the lack of need for the separation of an adsorbent after the process, the use of stabilized nanoparticles at a large scale is more economical and feasible [24,31].

Activated carbon has attracted great attention due to its high availability, low cost, high surface area, reusability, surface chemical properties and high pore volume [32,33]. However, commercial activated carbon is very costly. Thus, the scholars look for low-cost materials to replace the commercial activated carbon.

Activated carbon can be prepared from materials such as algae, coconut shells, corn, lignin, and so on [34]. The worn tires are extensively available in most areas. The production of activated carbon from these materials not only reduces the risks of their disposal but also produces a valuable product [35].

To our best knowledge, no reports have been presented regarding the performance of activated carbon produced from worn tires and the effect of stabilizing nanoparticles using plant extracts on activated carbon to remove Reactive Blue 19 (RB-19) and Reactive Black-5 (RB-5) dyes. Hence, its effectiveness in the removal of RB-19 and RB-5 was studied by different variables such as pH, reaction time, adsorbent dose, and initial dye concentration in synthetic solutions. Finally, the kinetics of the reactions and the adsorption isotherms were determined for the dye removal.

2. Materials and methods

2.1. Reagents, materials, and solutions

RB-19 and RB-5 dyes used in this study were prepared from Alvan Sabet Co., Hamedan, Iran. The general characteristics of both dyes have been presented in Table 1 [36,37]. In addition, H_2SO_4 and NaOH obtained from Merck Co., Germany, were applied to adjust the pH of the dye solution. It should be noted that in all stages of the experiments, double distilled water was used.
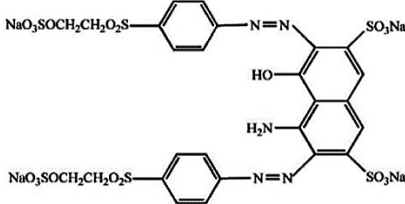
2.2. Instruments

The residual concentration of RB-19 and RB-5 dyes was measured by a UV/Vis spectrophotometer (HACH DR5000, USA) at the wavelengths 592 and 599 nm, respectively [36,38].

The characteristics of the samples including surface area, pore-volume, and pore size were determined by N_2 adsorption at 77 K using a Micromeritics (Australia) Tristar 3000 analyzer. Fourier transform infrared (FTIR) spectroscopy was performed to determine the functional groups at the adsorbent layers of the activated carbon by the PerkinElmer Spectrum FTIR spectrometer by KBr pallet technique in the range 450–4,000 cm^{-1} (FTIR, PerkinElmer, USA). X-ray diffraction (XRD) was employed to assess the phase structure of the samples by a Philips PAN-analytical diffractometer equipped with a Cu Ka X-ray source. Also, field emission scanning electron microscopy (FESEM) was used for determining the surface and morphological characteristics of the adsorbent at 10 keV acceleration voltage.

2.3. Activated carbon preparation

At first, the worn tires were crushed to a size fraction of 0.2–2.5 cm and then immersed in concentrated phosphoric acid for 48 h to be activated at ambient temperature. Afterward, rubbers were placed in a cylindrical steel reactor. The reactor than was placed in a programmable furnace model, HL40P controller. Furnace temperature reached 500°C at a rate of 5°C min^{-1} and then we remained at this temperature for 2 min. Next, the produced activated carbon was placed in an ultrasonic device at 37 kHz. The obtained

Table 1
Characteristics of RB-19 and RB-5 dyes

Name	Molecular structure	Molecular formula	Molecular weight
RB-19		$C_{22}H_{16}N_2O_{11}Na_2S_3$	626.54 g mol^{-1}
RB-5		$C_{26}H_{21}N_5Na_4O_{19}S_6$	991.82 g mol^{-1}

activated carbon was washed several times using deionized water to reach a pH of about 7. The washed specimens were completely dried for 2 h in an oven at 110°C. Finally, the activated carbon was stored in a container away from moisture for later use [24].

2.4. Preparation of ZnO nanoparticles by green synthesis method

In this study, the walnut shell was used to synthesize the ZnO nanoparticles in a greenway. To this end, 30 g of walnut shell was added to 500 mL of distilled water and placed on a magnetic stirrer at 300 rpm for 60 min at 80°C. After 1 h of extraction, the mixture was removed from the magnetic heater, cooled and then filtered through a vacuum pump. The obtained extract was mixed with ZnCl$_2$ (1 M) with a ratio of 2 to 3 and the synthesis of nanoparticles was seen by the formation of white clusters. Afterward, the mixture was poured into a graduated cylinder, washed 3 times with ethanol and then rinsed with double distilled water. In the next step, the residue was placed into a 50°C an oven to be completely dried. Then, to remove the interference from organic matters in the experiments, the nanoparticles were heated at room temperature for 2 h at 400°C in an electric furnace. Finally, the nanoparticles were stored for later use [24,39].

2.5. Loading ZnO nanoparticles on activated carbon

After AC preparation and ZnO synthesis, to produce the composite, first, 0.05 g of ZnO nanoparticles was added to 200 cc distilled water and was placed on a magnetic stirrer for 10 min to obtain a uniform solution. Next, 5 g of the activated carbon was added into the solution and placed again on a magnetic stirrer at 500 rpm for 10 h to complete the coating process. Then, the obtained composite was removed with a filter paper and washed several times with double-distilled water. Finally, the prepared composite was completely dried for 10 h in an oven at 95°C [24,40].

2.6. Adsorption experiments

The adsorption experiments were done by colored solutions with pH changes (3, 5, 7, 9 and 11), adsorbent value

(0.25, 0.5, 1, 1.5, and 2 g L^{-1}), dye concentration (50, 100, and 150 mg L^{-1}) and contact time (5, 10, 15, 30, 45, 60, and 75 min). During the process, the solution was stirred by a magnetic stirrer at 250 rpm. After the completion of the reaction time, centrifugation was done to isolate the solvent absorber at 3,000 rpm for 5 min. Then, the residual concentration of RB-19 and RB-5 were determined by the colorimetric method. Finally, the removal efficiency and dye absorbance in the adsorbent mass unit for RB-19 and RB-5 after the adsorption process was determined through Eqs. (1) and (2), respectively [41,42].

$$\text{Removal efficiency}\left(\%\right)\frac{C_0 - C_t}{C_0} \times 100 \tag{1}$$

$$\text{Adsorption capacity}\left(\text{mg g}^{-1}\right) = \frac{\left(C_0 - C_t\right) \times V}{M} \tag{2}$$

where C_0 and C_t are the initial and final concentrations of the dyes in solution (mg L^{-1}), V is the volume of the solution (L), and M is the mass of the adsorbent [43].

2.7. Determination of point-of-zero-charge (pzc)

One of the most important characteristics of the adsorbent is pH$_{zpc}$, showing the state of electrical charge dispersion on the adsorbent surface. To determine pH$_{zpc}$, 30 mL of a 0.1 M solution of sodium salt was poured into 100 mL 11 Erlenmeyer flasks and the pH of the solutions was adjusted between 2 and 12. Then, 0.05 g of the composite prepared in each of the flasks was added. Next, the solutions were placed on a shaker at a speed of 250 rpm for 48 h. Later, the final pH of the solutions was measured after the adsorption separation. Finally, pH$_{pzc}$ was determined after plotting the final pH change curve against the initial pH [44].

2.8. Determination of the efficiency of the adsorption process in removing dye from the actual wastewater

At this stage, the real wastewater was taken from a textile company and the composite performance was analyzed

for removing the dyes under the optimal conditions obtained from the artificial wastewater. To measure the dye, the adsorption curve was initially plotted using a spectrophotometer for the real centrifugal and filtered wastewater (to remove turbidity). The measurement was done at the maximum absorbance wavelength of 274 nm.

3. Results and discussion

3.1. Characterization of the adsorbent

3.1.1. Brunauer–Emmett–Teller analysis

Fig. 1a shows the nitrogen adsorption/desorption isotherms of the AC-ZnO composite and AC. According to the International Union of Pure and Applied Chemistry classification, the isotherms can be regarded as type IV indicating that the AC-ZnO composite and AC are porous and mesoporous. The hysteresis loop shows a capillary condensation step (p/p^0) between 0.5 and 0.9, illustrating the presence of mesoporous structure in both absorbents [45]. According to Fig. 1, it can be found that the Brunauer–Emmett–Teller (S_{BET}) of the AC-ZnO composite is more than that of the AC. The S_{BET} and pore volume of the adsorbents have been compiled in Table 2. The results obtained showed that the S_{BET} and total pure volume for the AC-ZnO composite and AC are 156.78 m^2 g^{-1}, 134.44 m^2 g^{-1}, 0.478 cm^3 g^{-1}, 0.421 cm^3 g^{-1}, respectively. The AC-ZnO composite and AC showed an average pore diameter of 2–3 nm, which can play an important role in the adsorption properties. On the one hand, the mesoporosity feature of materials allows that ions penetrate easier into their porous.

3.1.2. FTIR analysis

FTIR analysis provides structural information and combinations of sample functional groups. Fig. 2 shows the FTIR analysis of the activated carbon and AC-ZnO composite. The adsorption peak at 900–1,300 cm^{-1} is related to phosphorus-containing functional groups, where the activation of phosphoric acid during the preparation process was used [46]. Moreover, the peaks created at wavelengths of 400–800 cm^{-1} are related to the vibrations of Zn–O bonds in ZnO. The presence of the ZnO nanoparticles can be proved by the appearance of an adsorption band in 506 cm^{-1} [47]. The 2,800–3,000 cm^{-1} band with a peak at 2,859 cm^{-1} in the AC-ZnO composite is related to the presence of C–H alkanes [24]. The observed peak for the AC and AC-ZnO in the band 3,432 cm^{-1} can be related to the vibration of O–H in the H$_2$O molecule [48]. In addition, the observed peaks at 2,925 and 2,850 cm^{-1} bands showed the involvement of C–H and O–H (acidic group) of walnut shell extract in particle formation [49]. Polyphenols, acting as the main stabilizing factor for NPs, are observed from 3,200 to 3,500 cm^{-1} [47]. Some peaks in AC disappeared after ZnO coating and the disorder in the AC-ZnO spectrum decreased. Overall, the ZnO coating on AC was successful.

3.1.3. XRD analysis

The XRD pattern for the adsorbent at angle 2θ has been shown to determine the crystalline phase and structural properties of the nanoparticles. The results of this analysis showed that the peaks produced in 31.75°, 34.45°, 36.32°, 47.52°, 59.6°, 62.85°, 66.45°, 67.95°, and 69.15° degrees were
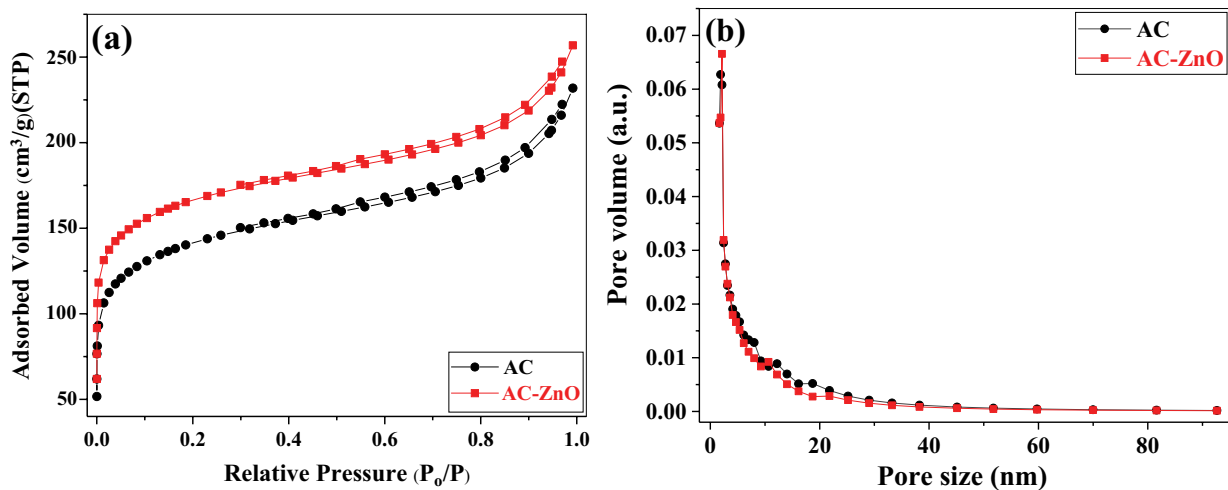

Fig. 1. N$_2$ adsorption–desorption isotherm (a) and the pore size distribution (b).

Table 2
BET specific surface area (S_{BET}), micropore specific surface area (S_{micro}), mesopore specific surface area (S_{meso}), total pore volume (V_{Total}), micropore volume (V_{micro}) and mesopore volume (V_{meso}) of AC and AC-ZnO

Material	S_{BET} (m^2 g^{-1})	S_{micro} (m^2 g^{-1})	S_{meso} (m^2 g^{-1})	V_{Total} (cm^3 g^{-1})	V_{micro} (cm^3 g^{-1})	V_{meso} (cm^3 g^{-1})	D_p (nm)
AC	134.44	70.79	63.65	0.421	0.1170	0.3040	2.23
AC-ZnO	156.78	84.61	72.17	0.478	0.1316	0.3467	2.61

Fig. 2. FTIR spectrum of AC and AC-ZnO composite samples.
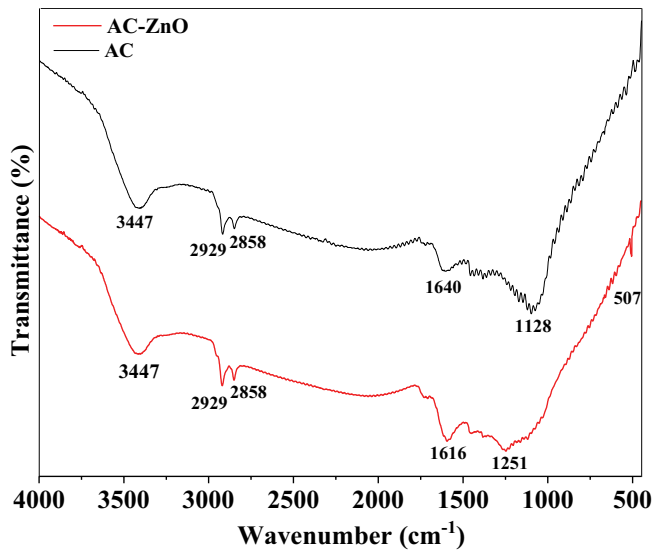

Fig. 3. XRD spectrum of AC and AC-ZnO adsorbents.

the indicators of ZnO in the structure of the synthesized adsorbent (Fig. 3). Moreover, the formation of sharpened and pulled peaks at angles 23.61°, 24.1°, and 26.5° was related to carbon, hence it could be stated that ZnO was successfully synthesized [50,51].

3.1.4. FESEM analysis

The surface and morphological characteristics of the activated carbon and AC-ZnO composite have been shown in Fig. 4. Fig. 4 shows the presence of pores and cavities on activated carbon with an asymmetric distribution. In addition, Fig. 4 indicates the nanoparticles of the ZnO particles as white particles. These nanoparticles were dispersed uniformly at an activated carbon level. The stabilization of the ZnO nanoparticles on the AC partially blocked the activated carbon porosity, which is probably because ZnO nanoparticles could not enter the internal voids of the activated carbon tissue; as a result, they remained on the outer surface
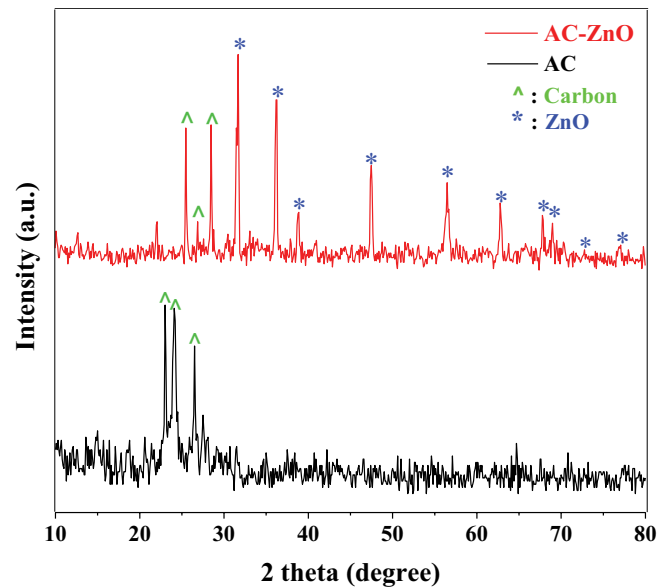
of the activated carbon. The FESEM image of the stabilized nanoparticles showed that the composite had porosity with a suitable surface and ZnO nanoparticles were well stabilized on the AC [18,50].

3.2. Effect of pH

The pH of aqueous solutions is one of the important parameters in controlling adsorption processes and the adsorption load level and ionic charge of dye molecules play a significant role in these processes [52]. Fig. 5 shows the effect of pH on the dye adsorption process. As can be observed with increasing pH from 3 to 11 the removal efficiency of the dyes decreased, which were from 71.58% to 47.24% for RB-19 and from 67.65% to 44.64% for RB-5. At this stage, pH = 3 was selected as the optimum value. At low pHs, the positive charge density increased on the
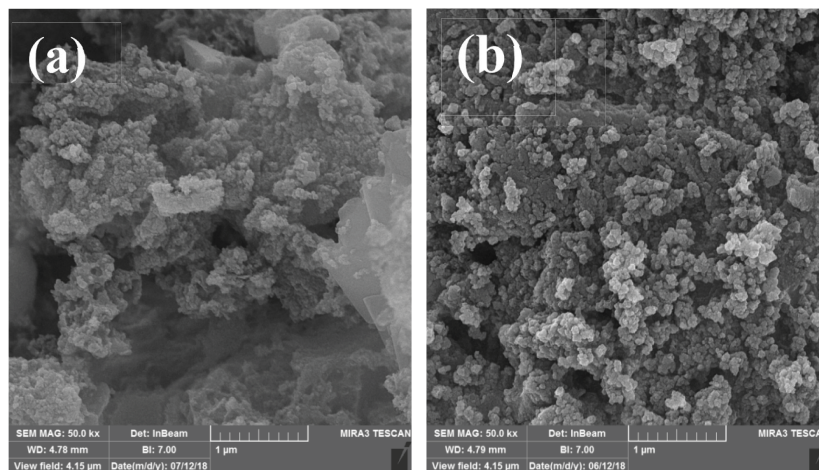

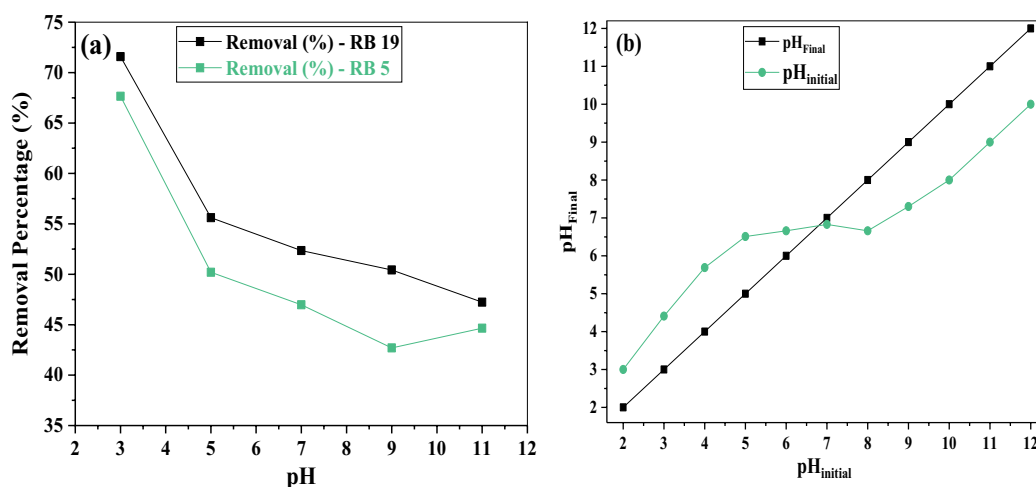Fig. 4. FESEM analysis of AC (a) and AC-ZnO (b).

Fig. 5. Effect of pH changes on the absorption efficiency of RB-19 and RB-5 using AC-ZnO (contact time: 30 min, initial dye concentration: 100 mg L^{-1}, solution temperature: 25°C, AC-ZnO dose: 1 g L^{-1}) (a) and pH$_{zpc}$ (b).

adsorbent surface and increased significantly between the adsorbent positive charge load and the electrochemical gravity molecule. Hence, the dye access to active sites increased and the dye distribution was facilitated. Furthermore, in alkaline pH, the number of sites with negative load increased, thereby decreasing the number of positive charge sites, which caused an increase in electrostatic repulsion [53,54].

Khaled et al. used an activated carbon of orange peel as an adsorbent to remove Direct N Blue-106 dye. The results illustrated that the removal efficiency of the dye increases with decreasing pH. The results were consistent with the present study [52]. Jamshidi et al. [55] obtained the same results in their study in which the removal of RB-19 dye by olive oil ash was evaluated. The observations were also in line with those of Fazlzadeh et al. [56].

3.3. Effect of adsorbent dose

Determination of absorbent dose is one of the most important parameters in adsorption given the economic considerations. Fig. 6 shows a change in the process of dye adsorption by the composite. The results illustrated that the removal rate in both dyes increased with raising adsorbent dose; it should be noted that the highest removal rate was observed at the dose of 2 g L^{-1}. When the dose was raised from 0.25 to 1.5 g L^{-1}, the removal efficiency rates of RB-19 and RB-5 increased from 31.41% to 96.19% and 28.66% to 71.37%, respectively. However, with an increasing dose of up to 2 g L^{-1}, the removal rate was negligible. Furthermore, the adsorption capacity reduced with an increase in dose, causing that the adsorption capacity of RB-19 and RB-5 to decline from 125.64 to 49.51 mg g^{-1} and 114.64 to 37.26 mg g^{-1} in doses from 0.25 to 2 g L^{-1}. Therefore, 1.5 g L^{-1} of the adsorbent was selected as the optimum dose. The number of positive sites enhances at the higher doses of the absorbent, increasing absorbency and strong propulsion [57]. At low doses of the absorbent, fewer active sites were available to the dye molecules, ending in a reduction in removal [58]. Although with an increase in adsorbent dose the removal efficiency increased due to the saturation of some sites on
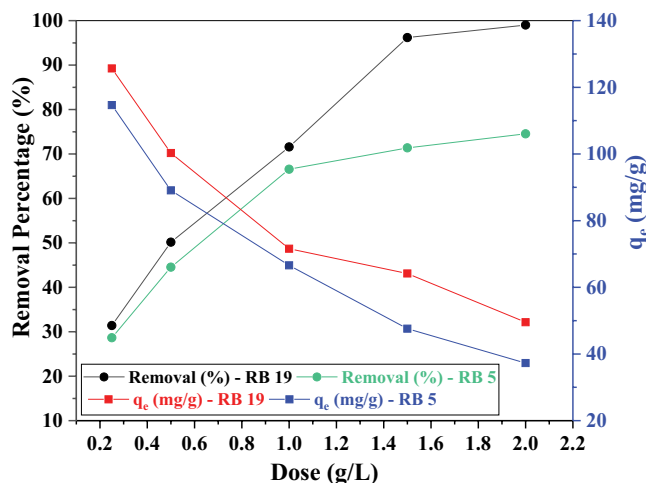

Fig. 6. Effect of adsorption dose changes on the efficiency of RB-19 and RB-5 dyes absorption using AC-ZnO composite (contact time: 30 min, pH: 3, initial dye concentration: 100 mg L^{-1}, solution temperature: 25°C).

the adsorbent surface, leading to a decrease in adsorption capacity [59]. The results of the research by Afkhami and Moosavi [60] showed that with an increase in adsorbent dose, the removal efficiency of the dye from the aqueous solution increased, which was in line with the findings of this study. Machado et al. [61] used multi-walled carbon nanotubes in the context of the adsorption of reactive red-dyed M-2BE in 2011; they reported similar results, and the results of the study were in line with those of the study by Nadejde et al. [62].

3.4. Effect of contact time

Another factor affecting dye removal is contact time. To examine the optimum contact time for the experiments, ranges of 50 to 150 mg L^{-1} and reaction time from 2 to 75 min were tested. As shown in Fig. 7, the composite efficiency
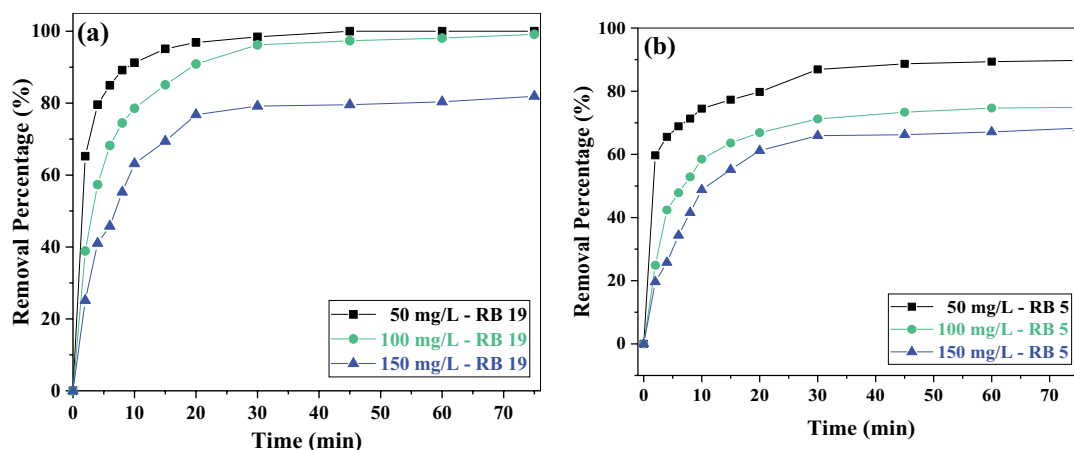
Fig. 7. Effect of contact time on the absorption efficiency of RB-19 (a) and RB-5(b) by using AC-ZnO composite (pH: 3, adsorbent doses: 1.5 g L^{-1}).

decreased in the removal of both dyes from a concentration of 50–150 mg L^{-1}. According to the results, the optimal contact time for the composite was 30 min. The adsorption of dye molecules on the outer surfaces of the composite started. However, due to the relative repulsion electrostatic force of the negative surface loads absorbed on the composite surface and the negative loads contained in the fluid mass, the emission rate of the contaminants within the porosity and, consequently, the adsorption rate decreased [63]. Moreover, firstly, the available levels for absorbing the pollutant on the composite were completely free; the contaminant was therefore in contact with the entire composite surface. As time passed, the available levels were reduced and the adsorption rate decreased as well [52]. These results were fully consistent with those of Regti et al. [64], who examined the removal of a dye using activated carbon. Furthermore, the results were similar to the observations in a study by Afshin et al. [42] who investigated the removal of a dye with an activated carbon prepared from filamentous algae.

3.5. Effect of dye concentration

As can be seen from Fig. 8, an increase in the initial concentration of RB-19 and RB-5 from 25 to 300 mg L^{-1} caused the adsorption efficiency to decrease from 100% to 47.35% and from 100% to 37.67%, respectively. With an increase of the initial dye concentration, due to the lack of active sites and the saturation of adsorption sites, the efficiency of removal was reduced because the adsorbent dose was constant [65]. Additionally, by increasing the initial dye content, the repulsion force created between the dye molecules disrupted the adsorption process and reduced the removal efficiency [43,66]. The results were completely consistent with the studies by Gupta et al. [53], who investigated the removal of dye blue 113 by an activated carbon from worn treads. Furthermore, Roosta et al. [67] obtained similar results in a study to remove dye with ZnS:Ni nanoparticles.

3.6. Adsorption isotherms

The changes in the initial concentrations of both isotherms were measured to examine the mechanism of
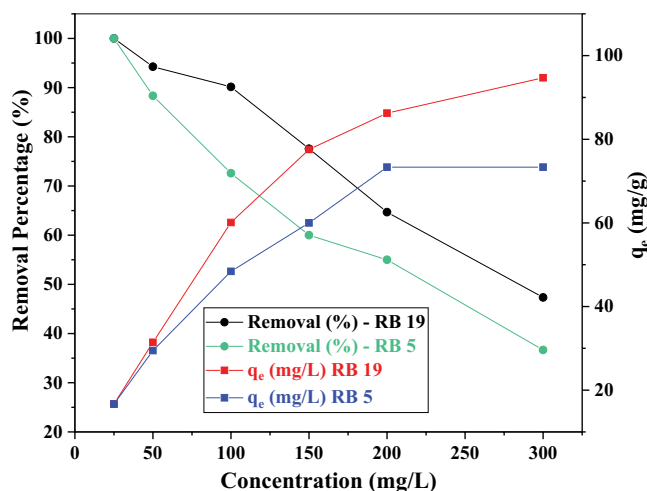

Fig. 8. Effect of changes in initial dye concentration on the absorption efficiency of RB-19 and RB-5 by using AC-ZnO composite (contact time: 40 min, pH: 3, adsorbent dosage: 1.5 g L^{-1}).

the equilibrium between the pollutant and composite. The adsorption data were analyzed using the Langmuir, Freundlich and Temkin isotherm equations [68,69].

The linear equations for the isotherms and kinetics have been given in Table 3 [31,70–72]. As the results in Fig. 9 and Table 4 show, the adsorption of RB-19 and RB-5 dyes using the present composite follows a regression coefficient of 0.9985 and 0.9656, respectively, of the Langmuir isotherm model. The Langmuir isotherm can be expressed in terms of a dimensionless constant named equilibrium parameter R_L, which is defined as follows:

$$R_L = \frac{1}{1 + k_L \times C_0} \tag{3}$$

where C_0 is the highest initial dye concentration (mg L^{-1}). The value of R_L indicates the type of the isotherm to be favorable ($0 < R_L < 1$), unfavorable ($R_L > 1$), linear ($R_L = 1$), or

Table 3
Linear equations of isotherm and kinetics

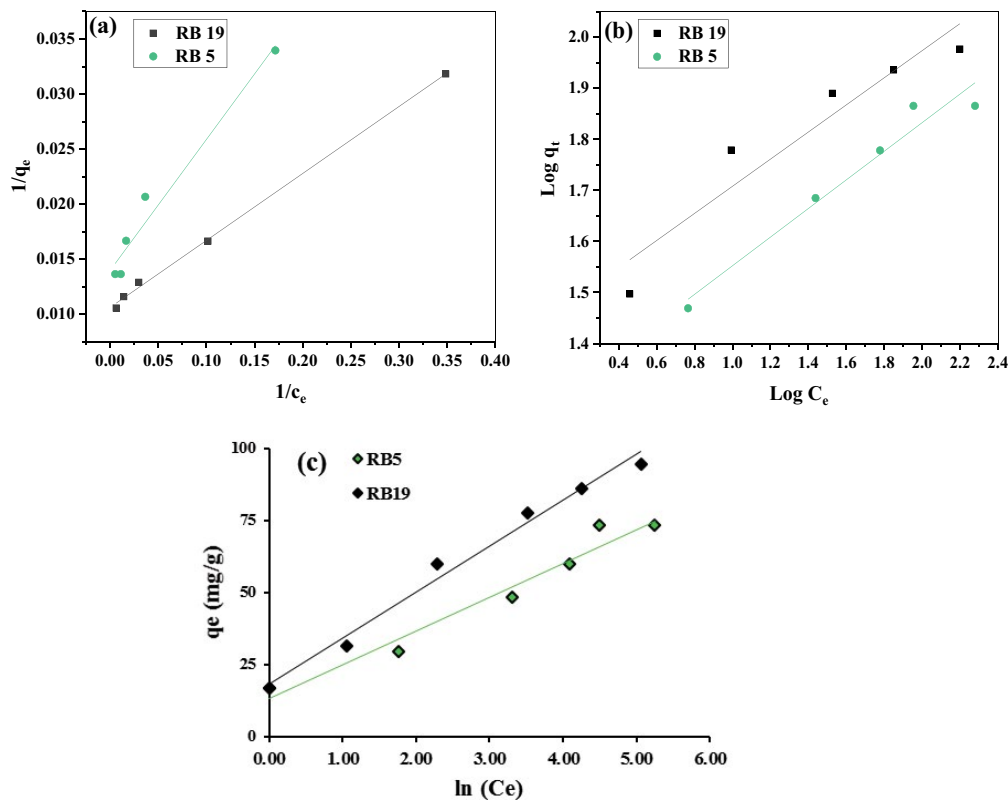|	Kinetic equations		Isothermal equations
Pseudo-first-order	$\log\left(q_e - q_t\right) = \log q_e - \left(\dfrac{k_1 t}{2.303}\right)$	Langmuir	$\dfrac{1}{q_e} = \dfrac{1}{k_l q_m c_e} + \dfrac{1}{q_m}$
Pseudo-second-order	$\dfrac{t}{q_e} = \dfrac{1}{\left(k_2 q_e^2\right)} + \left(\dfrac{1}{q_e}\right)t$	Freundlich	$\log q_e = \log k_f + \dfrac{1}{n}\log C_e$
Intraparticle diffusion	$q_t = K_{dif}\, t^{1/2} + C$	Temkin	$q_e = B_1 \ln K\, T + B_1 \ln C_e$

Fig. 9. Langmuir isotherm (a), Freundlich (b), and Temkin (c) in dye absorption on AC-ZnO composite.

irreversible ($R_L = 0$) [73,74]. The calculated values of R_L under different C_0 are found to be far lower than 1, showing the favorable adsorption of RB-5 and RB-19 by AC-ZnO.

Moreover, in this model, the value of $1/n$ was less than 1, showing that the adsorption of dyed material on the composite in lower concentrations was better than high concentrations of the dye and the process of adsorption was a chemical process [52,69]. The results accorded with the reports provided by other studies [50,55,75]. Table 5 shows the adsorption capacity of different types of adsorbent for RB-19 and RB-5. The maximum adsorption capacity of AC-ZnO for RB-19 and RB-5 was 94.33 and 71.42 mg g⁻¹, respectively. The results of the maximum adsorption capacity obtained indicated that the AC-ZnO composite had better performance than the other adsorbents used.

3.7. Adsorption kinetics

The rate of adsorption processes is critical in designing and evaluating adsorbents in the removal of dyes from dye solutions [76]. Fig. 10 presents the results of RB-19 and RB-5 dyes adsorption kinetics. The pseudo-first-order and second-order kinetic equations have been shown linearly (Table 3). In this equation, q_e and q_t were, respectively, adsorption capacities in equilibrium and time, as well as k_1 and k_2, the pseudo-first-rate and pseudo-second-order velocity coefficients. Considering the fixed coefficients and the correlation obtained in Table 6, it can be claimed that the process in question follows the pseudo-second-order kinetic model, and most of the adsorption was done by chemical absorption, confirming the results of the process isotherm [80]. Moreover, the results presented in Table 6 show that with

Table 4
Langmuir, Freundlich, and Temkin isotherm models at various concentrations

Isotherm	Parameters	Pollutant	
		RB-19	RB-5
Langmuir	q_m (mg g^{-1})	94.33	71.42
	K_L (L mg^{-1})	0.174	0.117
	R_L	0.103	0.145
	R^2	0.9985	0.9656
Freundlich	K_f ((mg g^{-1}) (mg L^{-1})$^{-1/n}$)	27.70	18.71
	n	3.766	3.57
	R^2	0.9058	0.9578
Temkin	B_1	15.99	11.75
	K_T (L mg^{-1})	0.935	0.921
	R^2	0.985	0.9341

increasing the concentration of RB-19 and RB-5 from 50 to 150 mg L^{-1}, the constant rate of reaction decreases from 0.032 to 0.003 and from 0.018 to 0.0029. This phenomenon shows that with increasing the concentration of pollutants, the adsorption rate decreased. The results of the isotherm of the process ($0.1n < 1$) illustrated that at the low concentrations of the pollutant, the process had a high efficiency. The results of Özcan et al. [36] regarding absorbing RB-19 dye using modified bentonite from aqueous solutions showed that the kinetics of this dye adsorption was consistent with the pseudo-second-order model. Ghaedi et al. [50] found similar results in their study on the removal of malachite green dye using a magnetic-activated carbon-oxide-zinc composite.

The intraparticle diffusion model proposed by Weber and Morris [81] was used to describe how the diffusion of RB-19 and RB-5 dye molecules onto AC-ZnO composite takes place. The diffusion model equations were shown linearly (Table 3), where k_{id} is the intra-particle diffusion rate constant. A plot of q_t vs. $t^{1/2}$ should be a straight line with a slope k_{id} and intercept C when the adsorption mechanism follows the intraparticle diffusion process. The values of the intercept give an idea about the thickness of the boundary layer, that is, the larger the intercept the greater is the boundary layer effect [82]. The values of characteristic parameters

in the intraparticle diffusion model, k_{id}, and C_i were determined through plotting q_t vs. $t^{1/2}$ (Fig. 11) (Table 7). From Fig. 11, it can be inferred that the lines did not pass through the origin, indicating that the intraparticle diffusion was not the only rate-limiting mechanism in the adsorption process; thus, some other mechanisms like liquid film diffusion may influence the adsorption kinetics.

3.8. Regeneration studies

The regeneration and recycling abilities of the adsorbents are important economically and the chemical method is mostly used in the retrieval of the adsorbents [83]. The disposing of spent adsorbents can be difficult because some of them could be hazardous and need to be incinerated and may be toxic, flammable or even explosive. The adsorption ability of the AC-ZnO composite for RB-19 and RB-5 dyes from aqueous solution was examined by using 0.1 M HNO3 and NaOH as a model. In the first stage, 1 g of the AC-ZnO composite was added in 100 mg L^{-1} of RB-19 and RB-5 dyes solution under the optimum conditions and, after the equilibrium time, the regeneration of the absorbent was investigated. These adsorption regeneration cycles were carried out up to five times (Fig. 12). After the regeneration, the spent adsorbents for the next regeneration stage were dried at 100°C for 12 h. Generally, it can be seen that the adsorption capacity of the composite decreased as the number of regeneration cycles increased. The AC-ZnO regeneration by 0.1M NaOH and 0.1 M HNO$_3$ was able to maintain an elimination efficiency of about 66.34% and 54.81% for RB-19 and equaled 47.84% and 43.69% for RB-5, respectively, even after the fifth cycle (Fig. 12). The high concentrations of NaOH and HNO$_3$ ions compete with RB-19 and RB-5 in active sites, and RB-19 and RB-5 were recovered from active sites and absorbent sites [83]. Given the proper recovery of AC-ZnO, its efficiency cost would be cost-effective. Moreover, it reduced secondary pollution in wastewater treatment [84].

3.9. Real wastewater samples

The results of dye removal from the actual samples have been shown in Fig. 13. Dye removal by the AC-ZnO composite was 76.22%. The properties of the actual wastewater were different from those of the synthetic samples. Some

Table 5
Comparison of maximum adsorption capacity (q_{max}) of various adsorbents for RB-19 and RB-5

| Adsorbent	Pollutant	q_{max} (mg g^{-1})	Reference
High lime fly ash	RB-5	7.18	[52]
Powdered activated carbon	RB-5	58.82	[52]
Brown seaweed, *Laminaria* sp.	RB-5	101.5	[52]
Banana peel powder	RB-5	49.2	[77]
Silica gel modified with 2,2'-(hexane-1,6-diylbis(oxy)) dibenzaldehyde	RB-19	72.99	[78]
Alumina/multi-walled carbon nanotubes	RB-19	3.67	[57]
Magnetic nanocomposite of Chitosan/SiO$_2$/CNTs	RB-19	97.08	[79]
AC-ZnO	RB-5	71.42	Present work
	RB-19	94.33	
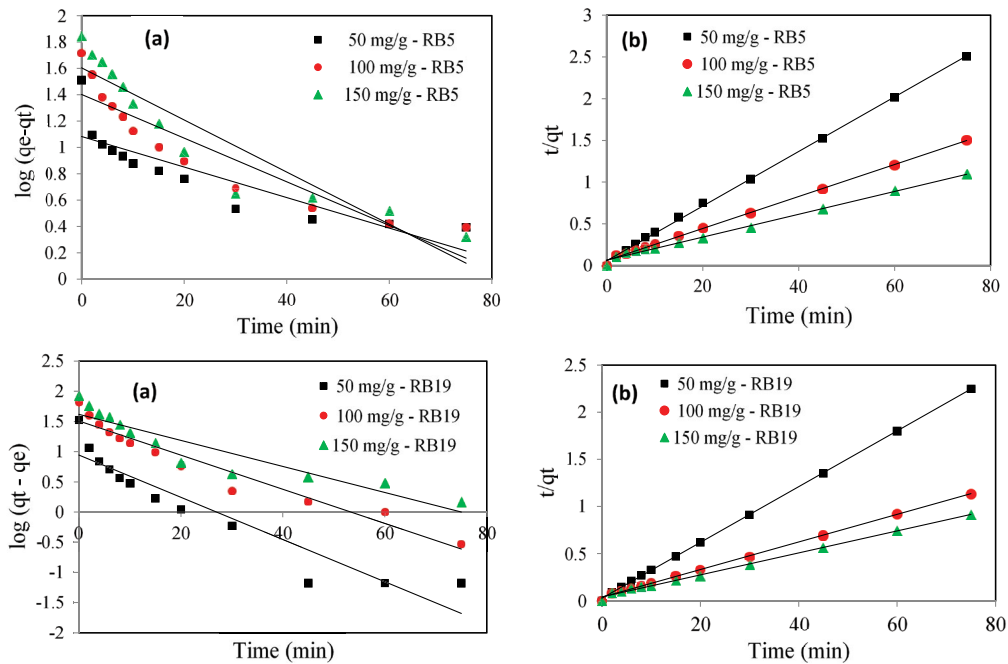
Fig. 10. Kinetic plots for the adsorption of RB-19 and RB-5 onto AC-ZnO composite at different dye concentration pseudo-first-order (a) and pseudo-second-order (b).
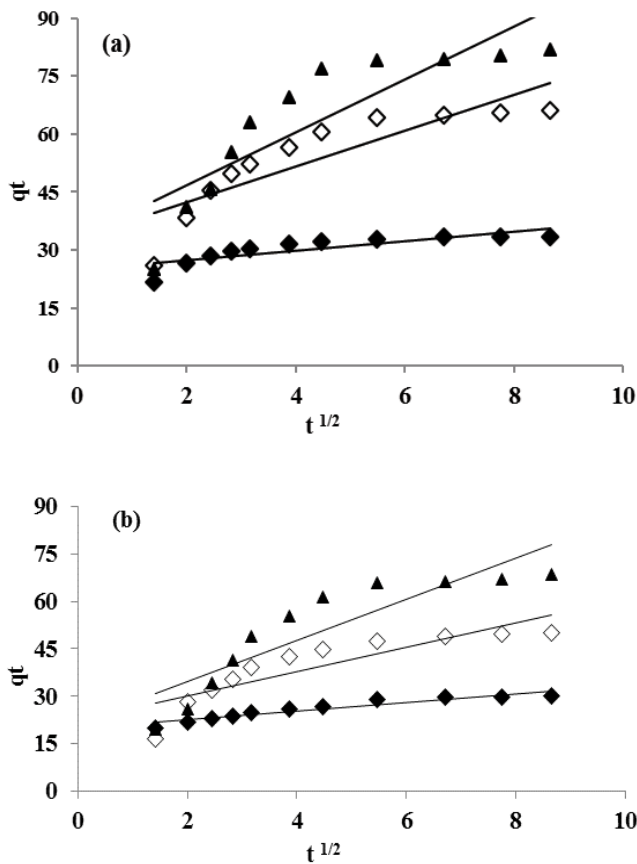

Fig. 11. Intraparticle diffusion plots for the adsorption of RB-19 (a) and RB-5 (b) dye onto AC-ZnO composite.

compounds like organic matter, in actual wastewater that may be removed by the adsorption process, thereby reducing the efficiency of the system in removing dye. Thus, it is expected to see a difference in the efficiency of the removal in actual and artificial samples. However, overall, these results showed the proper performance of the composite in removing dye from the actual samples.

4. Conclusions

The study indicated the significant efficiency of the AC-ZnO composite in the adsorption of RB-19 and RB-5 from aqueous solutions. XRD, BET, FESEM, and FTIR techniques confirmed the nature and structure of the composite. The results illustrated that an increase in reaction time and composite dosage increased the process efficiency. In contrast, an increase in pH and initial concentration of the dyes reduced the adsorption efficiency significantly. Under the optimal conditions: pH 3, initial dye concentration 100 mg L^{-1}, composite dose 1.5 g L^{-1} and reaction time 45 min, the removal efficiency rates for RB-19 and RB-5 were 97.36% and 73.36%, respectively. The results of the isotherm study and adsorption kinetics for both RB-19 and RB-5 showed that the adsorption process followed the Langmuir isotherm and pseudo-second-order kinetics. Furthermore, the results of the AC-ZnO composite regeneration with 0.1 M NaOH showed that high removal efficiency maintained after five times of reuse. Finally, it can be concluded that the studied composite can be used as an adsorbent with high access, efficient, and high-performance to remove dyes from the wastewater of different industries to evaluate the operating conditions of the adsorption process accurately.

Table 6
Kinetic parameters of dye absorption under optimal conditions and different concentrations

Concentration (mg L^{-1})	Pseudo-first-order				Pseudo-second-order		
	$q_{e,exp}$	$q_{e1,cal}$	k_1	R^2	$q_{e2,cal}$	k_2	R^2
50 (RB-5)	32.4	12.1	0.026	0.7521	30.48	0.018	0.999
100 (RB-5)	52.4	25.24	0.038	0.8523	52.08	0.0062	0.9981
150 (RB-5)	7.4	40.23	0.045	0.8766	72.99	0.0029	0.9942
50 (RB-19)	33.4	8.74	0.080	0. 877	33.78	0.032	0.9998
100 (RB-19)	66.4	32.26	0.065	0.9439	68.49	0.005	0.9987
150 (RB-19)	83.4	41.35	0.049	0.8642	85.47	0.003	0.9968

Table 7
Parameters of intraparticle diffusion kinetics for the adsorption of RB-19 and RB-5 dye onto AC-ZnO composite

Concentration (mg L^{-1})	Intraparticle diffusion equation constants					
	K		C		R^2	
	RB-5	RB-19	RB-5	RB-19	RB-5	RB-19
50	6.64	6.64	7.91	7.91	0.9863	0.9863
100	11.71	11.72	8.79	8.79	0.9119	0.9119
150	21.54	21.56	16.45	16.46	0.9568	0.9568

Fig. 13. AC-ZnO composite performance in real sewage.
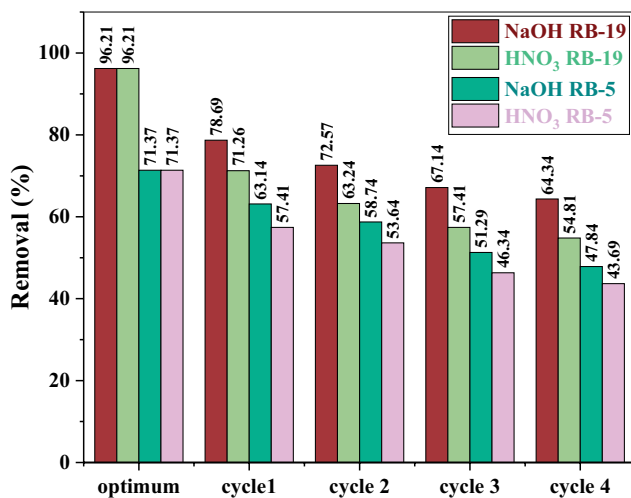
Fig. 12. Regeneration steps for AC-ZnO composites.

Acknowledgment

References

[1] W.A. Khanday, M. Asif, B.H. Hameed, Cross-linked beads of activated oil palm ash zeolite/chitosan composite as a bio-adsorbent for the removal of methylene blue and acid blue 29 dyes, Int. J. Biol. Macromol., 95 (2017) 895–902.

[2] R. Khosravi, M. Fazlzadehdavil, B. Barikbin, H. Hossini, Electro-decolorization of Reactive Red 198 from aqueous solutions using aluminum electrodes systems: modeling and optimization of operating parameters, Desal. Wat. Treat., 54 (2015) 3152–3160.

[3] A. Çelekli, M. Yavuzatmaca, H. Bozkurt, Kinetic and equilibrium studies on the adsorption of reactive red 120 from aqueous solution on *Spirogyra majuscula*, Chem. Eng. J., 152 (2009) 139–145.

[4] R. Khosravi, S. Hazrati, M. Fazlzadeh, Decolorization of AR18 dye solution by electrocoagulation: sludge production and electrode loss in different current densities, Desal. Wat. Treat., 57 (2016) 14656–14664.

[5] A.R. Rahmani, A. Shabanloo, M. Fazlzadeh, Y. Poureshgh, Investigation of operational parameters influencing in treatment of dye from water by electro-Fenton process, Desal. Wat. Treat., 57 (2016) 24387–24394.

[6] Mu. Naushad, Z.A. ALOthman, M. Rabiul Awual, S.M. Alfadul, T. Ahamad, Adsorption of rose Bengal dye from aqueous solution by amberlite Ira-938 resin: kinetics, isotherms, and thermodynamic studies, Desal. Wat. Treat., 57 (2016) 13527–13533.

[7] K. Sharafi, A.M. Mansouri, A.A. Zinatizadeh, M. Pirsaheb, Adsorptive removal of methylene blue from aqueous solutions by pumice powder: process modelling and kinetic evaluation, Environ. Eng. Manage. J., 14 (2015) 1067–1078.

[8] M. Hasan, A.L. Ahmad, B.H. Hameed, Adsorption of reactive dye onto cross-linked chitosan/oil palm ash composite beads, Chem. Eng. J., 136 (2008) 164–172.

[9] A.R. Rahmani, A. Shabanloo, M. Fazlzadeh, Y. Poureshgh, H. Rezaeivahidian, Degradation of Acid Blue 113 in aqueous

solutions by the electrochemical advanced oxidation in the presence of persulfate, Desal. Wat. Treat., 59 (2017) 202–209.

[10] A. Nasrullah, A.H. Bhat, A. Naeem, M.H. Isa, M. Danish, High surface area mesoporous activated carbon-alginate beads for efficient removal of methylene blue, Int. J. Biol. Macromol., 107 (2018) 1792–1799.

[11] L. Yang, Z. Wang, J.L. Zhang, Zeolite imidazolate framework hybrid nanofiltration (NF) membranes with enhanced perm-selectivity for dye removal, J. Membr. Sci., 532 (2017) 76–86.

[12] F. Abiri, N. Fallah, B. Bonakdarpour, Sequential anaerobic-aerobic biological treatment of colored wastewaters: case study of a textile dyeing factory wastewater, Water Sci. Technol., 75 (2017) 1261–1269.

[13] A. Almasi, A. Dargahi, A. Amrane, M. Fazlzadeh, M. Mahmoudi, A. Hashemian, Effect of the retention time and the phenol concentration on the stabilization pond efficiency in the treatment of oil refinery wastewater, Fresenius Environ. Bull., 23 (2014) 2541–2548.

[14] A. Othmani, A. Kesraoui, M. Seffen, The alternating and direct current effect on the elimination of cationic and anionic dye from aqueous solutions by electrocoagulation and coagulation flocculation, Euro-Mediterr. J. Environ. Integr., 2 (2017) 6.

[15] Z.G. Aguilar, E. Brillas, M. Salazar, J.L. Nava, I. Sirés, Evidence of Fenton-like reaction with active chlorine during the electrocatalytic oxidation of Acid Yellow 36 azo dye with Ir-Sn-Sb oxide anode in the presence of iron ion, Appl. Catal., B, 206 (2017) 44–52.

[16] T. Robinson, G. McMullan, R. Marchant, P. Nigam, Remediation of dyes in textile effluent: a critical review on current treatment technologies with a proposed alternative, Bioresour. Technol., 77 (2001) 247–255.

[17] J. Fan, D. Chen, N. Li, Q. Xu, H. Li, J. He, J. Lu, Adsorption and biodegradation of dye in wastewater with Fe_3O_4@MIL-100 (Fe) core-shell bio-nanocomposites, Chemosphere, 191 (2018) 315–323.

[18] K. Byrappa, A.K. Subramani, S. Ananda, K.M.L. Rai, M.H. Sunitha, B. Basavalingu, K. Soga, Impregnation of ZnO onto activated carbon under hydrothermal conditions and its photocatalytic properties, J. Mater. Sci., 41 (2006) 1355–1362.

[19] V.K. Gupta, P.J.M. Carrott, M.M.L. Ribeiro Carrott, Suhas, Low-cost adsorbents: growing approach to wastewater treatment—a review, Crit. Rev. Env. Sci. Technol., 39 (2009) 783–842.

[20] A.B. Albadarin, M.N. Collins, Mu. Naushad, S. Shirazian, G. Walker, C. Mangwandi, Activated lignin-chitosan extruded blends for efficient adsorption of methylene blue, Chem. Eng. J., 307 (2017) 264–272.

[21] R. Khosravi, A. Zarei, M. Heidari, A. Ahmadfazeli, M. Vosughi, M. Fazlzadeh, Application of ZnO and TiO_2 nanoparticles coated onto montmorillonite in the presence of H_2O_2 for efficient removal of cephalexin from aqueous solutions, Korean J. Chem. Eng., 35 (2018) 1000–1008.

[22] M. Moradi, A.M. Mansouri, N. Azizi, J. Amini, K. Karimi, K. Sharafi, Adsorptive removal of phenol from aqueous solutions by copper (cu)-modified scoria powder: process modeling and kinetic evaluation, Desal. Wat. Treat., 57 (2016) 11820–11834.

[23] Z. Heidarinejad, O. Rahmanian, M. Fazlzadeh, M. Heidari, Enhancement of methylene blue adsorption onto activated carbon prepared from Date Press Cake by low frequency ultrasound, J. Mol. Liq., 264 (2018) 591–599.

[24] M. Fazlzadeh, R. Khosravi, A. Zarei, Green synthesis of zinc oxide nanoparticles using *Peganum harmala* seed extract, and loaded on *Peganum harmala* seed powdered activated carbon as new adsorbent for removal of Cr(VI) from aqueous solution, Ecol. Eng., 103 (2017) 180–190.

[25] F. Ramezani, B. Kazemi, A. Jebali, Biosynthesis of silver nanoparticles by *Leishmania* sp., New Cellular Mol. Biotechnol. J., 3 (2013) 107–111.

[26] A. Matei, I. Cernica, O. Cadar, C. Roman, V. Schiopu, Synthesis and characterization of ZnO – polymer nanocomposites, Int. J. Mater. Form., 1 (2008) 767–770.

[27] I. De Angelis, F. Barone, A. Zijno, L. Bizzarri, M.T. Russo, R. Pozzi, F. Franchini, G. Giudetti, C. Uboldi, J. Ponti, F. Rossi, B. De Berardis, Comparative study of ZnO and TiO_2 nanoparticles: physicochemical characterisation and toxicological effects on human colon carcinoma cells, Nanotoxicology, 7 (2013) 1361–1372.

[28] L. Zhao, Y. Sun, J.A. Hernandez-Viezcas, A.D. Servin, J. Hong, G. Niu, J.R. Peralta-Videa, M. Duarte-Gardea, J.L. Gardea-Torresdey, Influence of CeO_2 and ZnO nanoparticles on cucumber physiological markers and bioaccumulation of Ce and Zn: a life cycle study, J. Agric. Food. Chem., 61 (2013) 11945–11951.

[29] S. Gunalan, R. Sivaraj, V. Rajendran, Green synthesized ZnO nanoparticles against bacterial and fungal pathogens, Prog. Nat. Sci.: Mater. Int., 22 (2012) 693–700.

[30] S. Iravani, Green synthesis of metal nanoparticles using plants, Green Chem., 13 (2011) 2638–2650.

[31] M. Ghaedi, M. Ghayedi, S.N. Kokhdan, R. Sahraei, A. Daneshfar, Palladium, silver, and zinc oxide nanoparticles loaded on activated carbon as adsorbent for removal of bromophenol red from aqueous solution, J. Ind. Eng. Chem., 19 (2013) 1209–1217.

[32] D. Bhatia, D. Datta, A. Joshi, S. Gupta, Y. Gote, Adsorption study for the separation of isonicotinic acid from aqueous solution using activated carbon/Fe_3O_4 composites, J. Chem. Eng. Data, 63 (2018) 436–445.

[33] M. Pirsaheb, Z. Rezai, A.M. Mansouri, A. Rastegar, A. Alahabadi, A.R. Sani, K. Sharafi, Preparation of the activated carbon from India shrub wood and their application for methylene blue removal: modeling and optimization, Desal. Wat. Treat., 57 (2016) 5888–5902.

[34] D. Mohan, C.U. Pittman Jr., Activated carbons and low cost adsorbents for remediation of tri- and hexavalent chromium from water, J. Hazard. Mater., 137 (2006) 762–811.

[35] E. Hoseinzadeh, A. Rahmani, Producing activated carbon from scrap tires by thermo-chemical method and evaluation its efficiency at removal racid black1 dye, Iran. J. Health Environ., 4 (2012) 428–438.

[36] A. Özcan, Ç. Ömeroğlu, Y. Erdoğan, A.S. Özcan, Modification of bentonite with a cationic surfactant: an adsorption study of textile dye Reactive Blue 19, J. Hazard. Mater., 140 (2007) 173–179.

[37] K.Z. Elwakeel, Removal of Reactive Black 5 from aqueous solutions using magnetic chitosan resins, J. Hazard. Mater., 167 (2009) 383–392.

[38] A.W.M. Ip, J.P. Barford, G. McKay, A comparative study on the kinetics and mechanisms of removal of Reactive Black 5 by adsorption onto activated carbons and bone char, Chem. Eng. J., 157 (2010) 434–442.

[39] Y. Rashtbari, Sh. Afshin, P. Pourali, M. Vahdat, Y. Poureshgh, M. Fazlzadeh, Investigating the efficiency of zero-valent iron nanoparticles (nZVI) produced by green synthesis in removing the acid black 1 from aqueous solution: a kinetic and isotherm study, Occup. Environ. Health J., 3 (2018) 250–264.

[40] M. Moradi, M. Soltanian, M. Pirsaheb, K. Sharafi, S. Soltanian, A. Mozafari, The efficiency study of pumice powder to lead removal from the aquatic environment: isotherms and kinetics of the reaction, J. Mazandaran Univ. Med. Sci., 23 (2014) 65–75.

[41] Y. Rashtbari, S. Hazrati, S. Afshin, M. Fazlzadeh, M. Vosoughi, Data on cephalexin removal using powdered activated carbon (PPAC) derived from pomegranate peel, Data Brief, 20 (2018) 1434–1439.

[42] S. Afshin, S.A. Mokhtari, M. Vosoughi, H. Sadeghi, Y. Rashtbari, Data of adsorption of Basic Blue 41 dye from aqueous solutions by activated carbon prepared from filamentous algae, Data Brief, 21 (2018) 1008–1013.

[43] F. de Sales Priscila, Z.M. Magriotis, M.A.L.S. Rossi, R.F. Resende, C.A. Nunes, Optimization by response surface methodology of the adsorption of Coomassie Blue dye on natural and acid-treated clays, J. Environ. Manage., 130 (2013) 417–428.

[44] M. Leili, M. Fazlzadeh, A. Bhatnagar, Green synthesis of nano-zero-valent iron from Nettle and Thyme leaf extracts and their application for the removal of cephalexin antibiotic from aqueous solutions, Environ. Technol., 39 (2018) 1158–1172.

[45] T.L. Silva, A.L. Cazetta, P.S.C. Souza, T. Zhang, T. Asefa, V.C. Almeida, Mesoporous activated carbon fibers synthesized

from denim fabric waste: efficient adsorbents for removal of textile dye from aqueous solutions, J. Cleaner Prod., 171 (2018) 482–490.

[46] M.-S. Miao, Q. Liu, L. Shu, Z. Wang, Y.-Z. Liu, Q. Kong, Removal of cephalexin from effluent by activated carbon prepared from alligator weed: kinetics, isotherms, and thermodynamic analyses, Process Saf. Environ. Prot., 104 (2016) 481–489.

[47] M. Ramesh, M. Anbuvannan, G. Viruthagiri, Green synthesis of ZnO nanoparticles using *Solanum nigrum* leaf extract and their antibacterial activity, Spectrochim. Acta, Part A, 136 (2015) 864–870.

[48] L.H. Huang, S. Zhou, F. Jin, J. Huang, N. Bao, Characterization and mechanism analysis of activated carbon fiber felt-stabilized nanoscale zero-valent iron for the removal of Cr(VI) from aqueous solution, Colloids Surf., A, 447 (2014) 59–66.

[49] K.S. Prasad, P. Gandhi, K. Selvaraj, Synthesis of green nano iron particles (GnIP) and their application in adsorptive removal of As(III) and As(V) from aqueous solution, Appl. Surf. Sci., 317 (2014) 1052–1059.

[50] M. Ghaedi, A. Ansari, M.H. Habibi, A.R. Asghari, Removal of malachite green from aqueous solution by zinc oxide nanoparticle loaded on activated carbon: kinetics and isotherm study, J. Ind. Eng. Chem., 20 (2014) 17–28.

[51] W.J. Xu, Q.L. Zhao, R.F. Wang, Z.M. Jiang, Z.Z. Zhang, X.W. Gao, Z.F. Ye, Optimization of organic pollutants removal from soil eluent by activated carbon derived from peanut shells using response surface methodology, Vacuum, 141 (2017) 307–315.

[52] A. Khaled, A. El Nemr, A. El-Sikaily, O. Abdelwahab, Removal of Direct N Blue-106 from artificial textile dye effluent using activated carbon from orange peel: adsorption isotherm and kinetic studies, J. Hazard. Mater., 165 (2009) 100–110.

[53] V.K. Gupta, B. Gupta, A. Rastogi, S. Agarwal, A. Nayak, A comparative investigation on adsorption performances of mesoporous activated carbon prepared from waste rubber tire and activated carbon for a hazardous azo dye—Acid Blue 113, J. Hazard. Mater., 186 (2011) 891–901.

[54] A.S. Özcan, A. Özcan, Adsorption of acid dyes from aqueous solutions onto acid-activated bentonite, J. Colloid Interface Sci., 276 (2004) 39–46.

[55] B. Jamshidi, M.H. Ehrampoush, M. Dehvari, Utilization of olive kernel ash in removal of RB-19 from synthetic textile wastewater, J. Environ. Treat. Technol., 1 (2013) 151–157.

[56] M. Fazlzadeh, H. Abdoallahzadeh, R. Khosravi, B. Alizadeh, Removal of Acid Black 1 from aqueous solutions using Fe_3O_4 magnetic nanoparticles, J. Mazandaran Univ. Med. Sci., 26 (2016) 174–186.

[57] M. Malakootian, H.J. Mansoorian, A. Hosseini, N. Khanjani, Evaluating the efficacy of alumina/carbon nanotube hybrid adsorbents in removing Azo Reactive Red 198 and Blue 19 dyes from aqueous solutions, Process Saf. Environ. Prot., 96 (2015) 125–137.

[58] M. Jamshidi, M. Ghaedi, K. Dashtian, A.M. Ghaedi, S. Hajati, A. Goudarzi, E. Alipanahpour, Highly efficient simultaneous ultrasonic assisted adsorption of brilliant green and eosin B onto ZnS nanoparticles loaded activated carbon: artificial neural network modeling and central composite design optimization, Spectrochim. Acta, Part A, 153 (2016) 257–267.

[59] E. Hoseinzadeh, A.R. Rahmani, G. Asgari, M.T. Samadi, G. Roshanaei, M.R. Zare, Application of adsorption process by activated carbon derived from scrap tires for Pb^{+2} removal from aqueous solutions, J. Birjand Univ. Med. Sci., 20 (2013) 45–57.

[60] A. Afkhami, R. Moosavi, Adsorptive removal of Congo red, a carcinogenic textile dye, from aqueous solutions by maghemite nanoparticles, J. Hazard. Mater., 174 (2010) 398–403.

[61] F.M. Machado, C.P. Bergmann, T.H. Fernandes, E.C. Lima, B. Royer, T. Calvete, S.B. Fagan, Adsorption of Reactive Red M-2BE dye from water solutions by multi-walled carbon nanotubes and activated carbon, J. Hazard. Mater., 192 (2011) 1122–1131.

[62] C. Nadejde, M. Neamtu, R.J. Schneider, V.-D. Hodoroaba, G. Ababei, U. Panne, Catalytical degradation of relevant pollutants from waters using magnetic nanocatalysts, Appl. Surf. Sci., 352 (2015) 42–48.

[63] R.F. Fard, M.E.K. Sar, M. Fahiminia, N. Mirzaei, N. Yousefi, H.J. Mansoorian, N. Khanjani, S. Rezaei, S.K. Ghadiri, Efficiency of multi walled carbon nanotubes for removing Direct Blue 71 from aqueous solutions, Eurasian J. Anal. Chem., 13 (2018), doi: https://doi.org/10.29333/ejac/85010.

[64] A. Regti, M.R. Laamari, S.-E. Stiriba, M. El Haddad, Use of response factorial design for process optimization of basic dye adsorption onto activated carbon derived from Persea species, Microchem. J., 130 (2017) 129–136.

[65] A. Amouei, H.A. Asgharnia, K. Karimian, Y. Mahdavi, D. Balarak, S.M. Ghasemi, Optimization of dye Reactive Orange 16 (RO16) adsorption by modified sunflower stem using response surface method from aqueous solutions, 14 (2016) 813–826.

[66] M. Arthy, M.P. Saravanakumar, Isotherm modeling, kinetic study and optimization of batch parameters for effective removal of Acid Blue 45 using tannery waste, J. Mol. Liq., 187 (2013) 189–200.

[67] M. Roosta, M. Ghaedi, A. Daneshfar, S. Darafarin, R. Sahraei, M.K. Purkait, Simultaneous ultrasound-assisted removal of sunset yellow and erythrosine by ZnS:Ni nanoparticles loaded on activated carbon: optimization by central composite design, Ultrason. Sonochem., 21 (2014) 1441–1450.

[68] G. Zolfaghari, A. Esmaili-Sari, M. Anbia, H. Younesi, S. Amirmahmoodi, A. Ghafari-Nazari, Taguchi optimization approach for Pb(II) and Hg(II) removal from aqueous solutions using modified mesoporous carbon, J. Hazard. Mater., 192 (2011) 1046–1055.

[69] S. Kholghi, K.H. Badii, S.H. Ahmadi, Bio-sorption isotherm and kinetic study of Acid Red 14 from aqueous solution by using *Azolla A. Filiculodes*, J. Color Sci. Technol., 6 (2013) 337–346.

[70] L.J. Zhang, P. Hu, J. Wang, R.H. Huang, Adsorption of Amido Black 10B from aqueous solutions onto Zr (IV) surface-immobilized cross-linked chitosan/bentonite composite, Appl. Surf. Sci., 369 (2016) 558–566.

[71] A.A. Alqadami, Mu. Naushad, Z.A. Alothman, A.A. Ghfar, Novel metal–organic framework (MOF) based composite material for the sequestration of U(VI) and Th(IV) metal ions from aqueous environment, ACS Appl. Mater. Interfaces, 9 (2017) 36026–36037.

[72] S. Afshin, Y. Rashtbari, M. Shirmardi, M. Vosoughi, A. Hamzehzadeh, Adsorption of Basic Violet 16 dye from aqueous solution onto mucilaginous seeds of *Salvia sclarea*: kinetics and isotherms studies, Desal. Wat. Treat., 161 (2019) 365–375.

[73] A.H. Mahvi, M.J. Mohammadi, M. Vosoughi, A. Zahedi, B. Hashemzadeh, A. Asadi, S. Pourfadakar, Sodium dodecyl sulfate modifed-zeolite as a promising adsorbent for the removal of natural organic matter from aqueous environments, Health Scope, 5 (2016) 11–18.

[74] M.O. Borna, M. Pirsaheb, M.V. Niri, R.K. Mashizie, B. Kakavandi, M.R. Zare, A. Asadi, Batch and column studies for the adsorption of chromium(VI) on low-cost *Hibiscus Cannabinus kenaf*, a green adsorbent, J. Taiwan Inst. Chem. Eng., 68 (2016) 80–89.

[75] Z.A. Al-Othman, R. Ali, Mu. Naushad, Hexavalent chromium removal from aqueous medium by activated carbon prepared from peanut shell: adsorption kinetics, equilibrium and thermodynamic studies, Chem. Eng. J., 184 (2012) 238–247.

[76] S. Chatterjee, T. Chatterjee, S.H. Woo, Influence of the polyethyleneimine grafting on the adsorption capacity of chitosan beads for Reactive Black 5 from aqueous solutions, Chem. Eng. J., 166 (2011) 168–175.

[77] V.S. Munagapati, V. Yarramuthi, Y. Kim, K.M. Lee, D.-S. Kim, Removal of anionic dyes (Reactive Black 5 and Congo Red) from aqueous solutions using Banana Peel Powder as an adsorbent, Ecotoxicol. Environ. Saf., 148 (2018) 601–607.

[78] A. Banaei, S. Samadi, S. Karimi, H. Vojoudi, E. Pourbasheer, A. Badiei, Synthesis of silica gel modified with 2,2'-(hexane-1,6-diylbis(oxy)) dibenzaldehyde as a new adsorbent for the removal of Reactive Yellow 84 and Reactive Blue 19 dyes from aqueous solutions: equilibrium and thermodynamic studies, Powder Technol., 319 (2017) 60–70.

[79] M. Abbasi, Synthesis and characterization of magnetic nanocomposite of chitosan/SiO$_2$/carbon nanotubes and its

application for dyes removal, J. Cleaner Prod., 145 (2017) 105–113.

[80] B. Kakavandi, J.A. Jafari, R.R. Kalantary, S. Nasseri, A. Ameri, A. Esrafily, Synthesis and properties of Fe_3O_4-activated carbon magnetic nanoparticles for removal of aniline from aqueous solution: equilibrium, kinetic and thermodynamic studies, J. Environ. Health Sci. Eng., 10 (2013) 19.

[81] W.J. Weber, J.C. Morris, Kinetics of adsorption on carbon from solution, J. Sanitary Eng. Div., 89 (1963) 31–60.

[82] N. Kannan, M.M. Sundaram, Kinetics and mechanism of removal of methylene blue by adsorption on various carbons—a comparative study, Dyes Pigm., 51 (2001) 25–40.

[83] V.K. Gupta, R. Kumar, A. Nayak, T.A. Saleh, M.A. Barakat, Adsorptive removal of dyes from aqueous solution onto carbon nanotubes: a review, Adv. Colloid Interface Sci., 193 (2013) 24–34.

[84] H.I. Chieng, L.B. Lim, N. Priyantha, Enhancing adsorption capacity of toxic malachite green dye through chemically modified breadnut peel: equilibrium, thermodynamics, kinetics and regeneration studies, Environ. Technol., 36 (2015) 86–97.